COB-2021-0766

Performance of the NREL Phase VI wind turbine blades with Wavy Leading Edge designed proportional to the blade local chord

Juan Antonio Flores-Mezarina
Andressa Caroline Rodrigues Garcia
Hernan Darío Ceron-Muñoz
University of São Paulo, São Carlos School of Engineering, São Carlos, Brazil
juan.flores@usp.br; agarcia@usp.br; hernan@sc.usp.br

Abstract. The Wavy Leading Edge (WLE) is a passive control flow device inspired on the Humpback whale pectoral flippers. It generates counter-rotating vortices at the leading edge that re-energize the flow and prevents its abrupt detachment. This delays stall and increases lift after stall in diverse degrees, according to the WLE governing parameters: amplitude and wavelength. Horizontal Axis Wind Turbines (HAWT) are designed to operate under the most probable wind speeds and transform the wind kinetic energy into useful energy. However, the complex environmental conditions limit their operational range. Since the HAWT operational range includes high wind speeds at which their blades operate mostly in stall regime, it is valid to take into account the WLE on their design. Studies on the performance effects of the WLE on the NREL Phase VI wind turbine blades showed that it degrades the blade performance at the turbine design wind speed (10 m/s) and significantly enhances it at higher speeds (>10 m/s). In these studies, the WLE dimensions were set constant along the entire blade span, while the blade chord decreases towards its tip. Under this approach, the WLE amplitude and wavelength ratios vary along the entire blade and turn the WLE configuration optimum only at a specific section of the blade span. In this study, the blade chord reduction was taken in account when designing the WLE. As result its amplitude and wavelength ratios are set constant to the blade local chord along the entire blade. The analysis was carried out using CFD simulations at different wind speeds. Under this approach, the blade performance is less degraded by the WLE at its design wind speed and it is still significantly increased at high wind speeds. Therefore, the wind turbine optimum operational range can be extended and adapted to different locations only by adapting the blades WLE ratios.

Keywords: Wavy Leading Edge, WLE, Leading Edge Protuberances, NREL Phase VI Wind Turbine, Wind Energy

1. Introduction

The Humpback whale complex feeding maneuvers have inspired several studies. It was found that the bumps on the leading edge of their pectoral flippers act as passive control flow devices that increase their hydrodynamic performance at high angles of attack (Fish and Battle, 1995). These bumps inspired the Wavy Leading Edge (WLE), a device that replies the bumps with a sinusoidal function. Tested on rectangular wings, it was shown that the WLE re-energizes the flow over their upper face, this delays the stall angle and increases lift after stall (Miklosovic *et al.*, 2004). CDF pressure contours and flow visualizations tests showed that: as the flow reaches first the wave peaks, the pressure over them is higher than over the wave valleys (Dropkin *et al.*, 2012). This pressure difference creates a span-wise velocity component that generates counter-rotating vortices at each peak side (Custodio, 2007). Studies on the aerodynamic effects of varying of the WLE governing parameters, Amplitude (A) and Wavelength (λ), showed that: Amplitude increment degrades the lift slope before stall and maximum lift; on the other hand, it also turns stall smoother and increases lift after stall. Wavelength has fewer effects; however, its reduction increases the lift performance before stall and the maximum lift, it also contributes to a smoother stall transition (Johari *et al.*, 2007; Hansen *et al.*, 2011). The WLE counter-rotating vortices also perform as small fences that reduce the span-wise flow intensity. This contributes to reduce the induced drag and the tip vortex intensity (Bolzon *et al.*, 2016).

Wind turbines transform the wind kinetic energy into torque to generate useful energy. Horizontal Axis Wind Turbines (HAWT) performance is limited by the wind direction and velocity. To maximize the wind energy harvesting, the HAWT blades operational range extends from the most probable to both lower and higher wind speeds. Since high wind speeds can endanger the wind turbine components and blades, active or passive control mechanisms are used to avoid any damage. The first one uses mobile components to pitch the wind turbine blade either to feather condition, or to induce the blade stall. The second one uses the blade twist angle to gradually induce stall from the blade root to the tip if the wind speed exceeds the design values. The active control mechanism is advantageous because it allows higher power production, while the passive one is advantageous because its simplicity(Manwell *et al.*, 2010; Letcher, 2017).

Since the passive stall controlled blades are exposed to stall and deep stall conditions, the WLE has arisen as a convenient device to increase its power production at high wind speeds.

The NREL Phase VI wind turbine is a relatively simple, in comparison to other modern wind turbines. It was designed with a single airfoil (S809) and a linearly decreasing chord. Its two blades have $5.029\ m$ of radius and $3°$ of fixed pitch angle, its rotating speed is fixed at $72\ RPM$, and it reaches its best performance at $10\ m/s$ wind speed (Hand *et al.*, 2001). All these features turn the NREL Phase VI wind turbine blade suitable to research the WLE effects on wind turbines. It was found that the WLE has different effects on the wind turbine performance, according to the wind speed . While at $7\ m/s$ or lower wind speeds there is no significant effect on performance, at $10\ m/s$ it is degraded up to 23% or 50%, according to the amplitude and wavelength configurations in each study. On the other hand, at $15\ m/s$ the blade performance is similar to the base blade and even 26% higher. At $20\ ms$ it is enhanced up to 26% (Zhang and Wu, 2012; Abate *et al.*, 2019). On these studies, the WLE was designed in function to a fixed chord. This keeps the wave dimensions constant along the blade span while the amplitude and wavelength ratios variate in function to the local chord, which causes the WLE configuration to be optimal only at a blade section. The WLE fence effect is shown at high wind speeds ($> 10\ m/s$), it limits the spreading of the flow detachment from the blade root to the tip. The blade performance increment reported at high wind speeds is caused by a higher attached flow area towards the blade tip.In this study, the effects of the WLE designed with Amplitude and Wavelength ratios in function to the root and local chord on the NREL Phase VI wind turbine blade performance are assessed. The analysis was carried out on the finite element based software ANSYS® CFX.

2. Methodology

2.1 Geometry

To carry out the tests of this exploratory study, a set of five blades was deigned: a base blade with smooth leading edge, two WLE blades with Amplitude and Wavelength ratios set in function to the root chord (c_{root}), and two WLE blades with the same ratios set in function to the blade local chord (c_{loc}). The WLE was generated by displacing the original airfoil coordinates according to the wave amplitude along the entire blade span (Johari *et al.*, 2007; Custodio, 2007). To avoid uneven transitions on the geometry and isolate the effects of the wave size, the last wave valley was aligned to the blade tip; besides, the blade leading edge is smooth up to the wave fist inflection point. The blade nomenclatures and WLE ratios are shown in table 1, notice the variation of the WLE amplitude and wavelength ratios under both approaches, also illustrated in figure 1. Note that blade N-rt1 and N-loc1 have a similar WLE configuration at the blade root. However, at the blade tip blade N-rt1 ratios in function to the local chord have doubled and there the blades N-rt2 and N-loc1 have similar wave Amplitude.
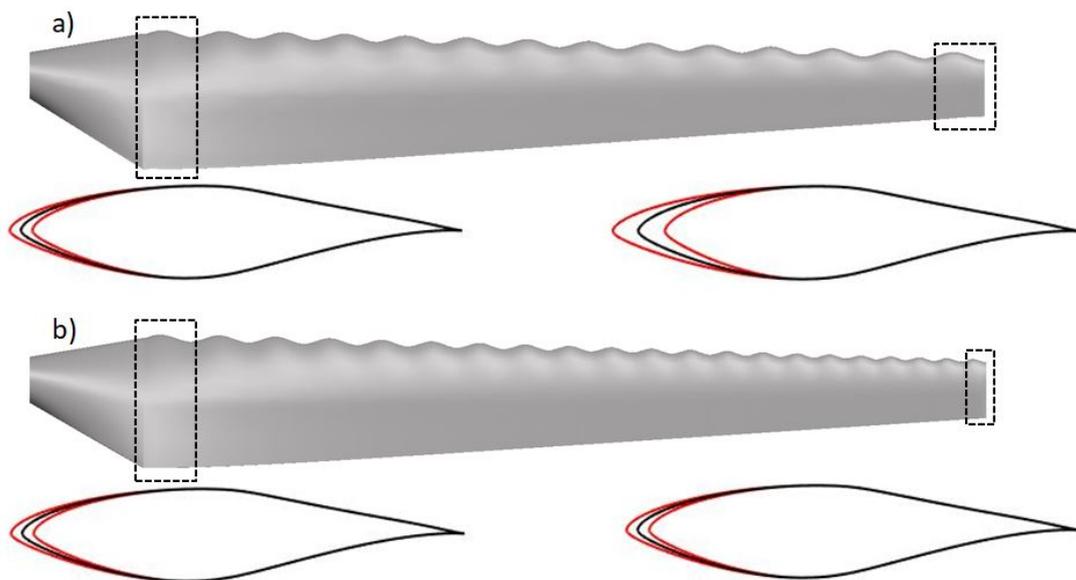

Figure 1: Amplitude and wavelength ratios in function to a) the root chord, and b) the local chord.

Nomenclature	At the blade Root		At the blade Tip	
	A	λ	A	λ
NREL	-	-	-	-
N-rt1	4.5	43	9.3	88.5
N-rt2	2.1	30	4.3	61.8
N-loc1	4.5	43	4.5	43
N-loc2	2.1	30	2.1	30

Table 1: Blades nomenclature and WLE ratios as percentage of the local chord at the blade root and tip. Blades N-rt1 and N-rt2 follow the the literature approach, and blades N-loc1 and N-loc2 use the one proposed in this study.

2.2 Numerical Analysis

The numerical analysis was carried in the commercial software ANSYS® CFX solver. The domain is composed by a static external domain and a internal rotating sub-domain. To save computational cost during the meshing process, both domains are composed by unstructured tetrahedral elements. The only structure elements are in the first 25 layers over the blade surface, small enough to reach $y+ \approx 1$. Domain and sub-domain boundary condition was set as frozen-rotor general grid interface. The domain dimensions and boundary layer conditions are shown in table 2, and illustrated in figure 2. Due to its overall little lift, drag and momentum error, the k-ω SST turbulent model (Menter *et al.*, 2003) was used in the solver. The turbine tower and nacelle were not included in the simulations because of their little aerodynamic effects on the turbine blades (Song and Perot, 2015; Zhang and Wu, 2012; Sørensen *et al.*, 2002; Sobotta *et al.*, 2016).

Boundary	Distance	Condition
Inlet	$2.4R$	Inlet
Outlet	$6.4R$	Opening
External Wall	$7R$	Opening
Side Wall	-	Periodic Symmetry

Table 2: Domain dimensions, set in function to the blade radius R, and boundary conditions.
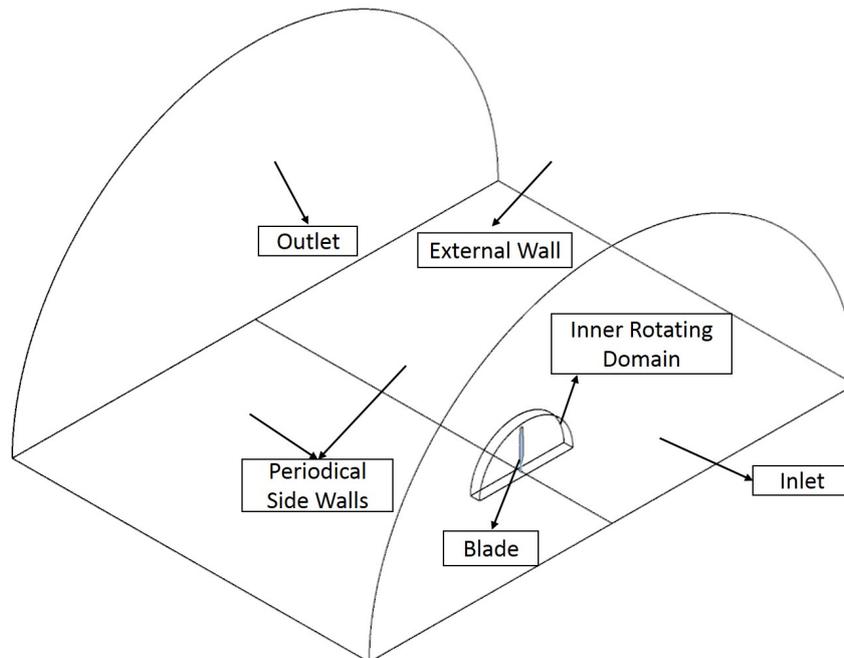

Figure 2: Domain of the numerical analysis.

3. Results

Figure 3 shows the torque for all the blades tested. At $10 \ m/s$, there is no significant difference between blades N-rt1 and N-loc1, the blades with higher A and λ; both reduce torque nearly 13%. On the other hand, blades N-rt2 and N-loc2 have a notorious difference in performance. While blade N-rt2 reduces torque almost 19%, blade N-loc2 reduces it only 8.5%. At $15 \ m/s$, the difference between blades N-rt1 and N-loc1 is still negligible, both improve torque around 19%. Blades N-rt2 and N-loc2 improve torque 11% and 7% respectively, the difference between them was reduced and the blade N-rt2 has better performance. At $20 \ m/s$, blade N-rt1 outperforms with 25% torque increase while blade N-loc1 reaches almost 15%. Blades N-rt2 and N-loc2 perform similarly and increase torque nearly 7%. Similar results at 15 and $20 \ m/s$ were reported in previous studies (Zhang and Wu, 2012; Abate and Mavris, 2018; Abate *et al.*, 2019). However; the torque reduction at the blade design speed, $10 \ m/s$, was more severe. This represented a potential disadvantage of using the WLE on HAWT, since the blade performance was reduced at the most probable wind speed.
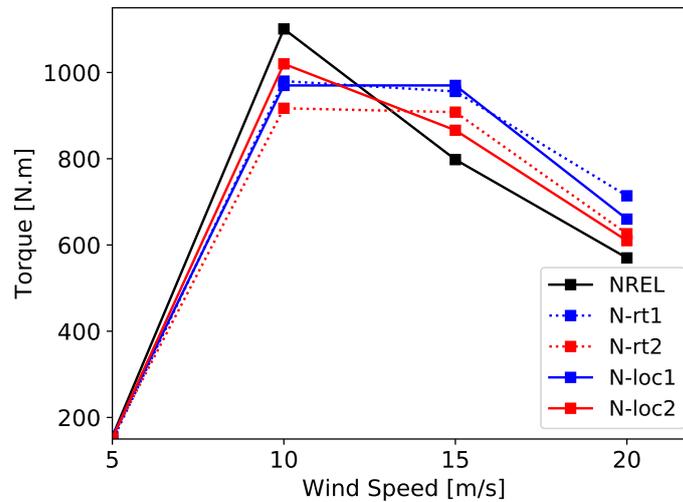

Figure 3: Torque results, the same colors are used for the blades that have the same A and λ values at the root. The solid lines correspond to the blades with A and λ set in function to the local chord while the dashed lines to the ones with A and λ set in function to the root chord.

Figure 4 shows the velocity streamlines over the blades at $10 \ m/s$. Blades N-rt1 and N-loc1, that have the biggest WLE dimensions perform similarly. Although flow is re-energized by the WLE, at the blade root the attached flow area is similar to the base blade. At the transition to the blade tip, flow is is chaotic and the flow attached area is smaller. Blade N-rt2 also has an attached flow area even smaller at the blade root and at the transition to the blade tip. On the other hand; flow over the N-loc2 blade has a more gradual behavior. Even though its detached flow area at the blade root is larger than over all the blades, it spreads more gradually towards the blade tip, which seems to correspond to the gradual size decrease of the WLE towards the blade tip. At the transition to the blade tip, the attached flow area is larger than over all the WLE blades. Flow at the blade tip is fully attached along the chord over all the blades.
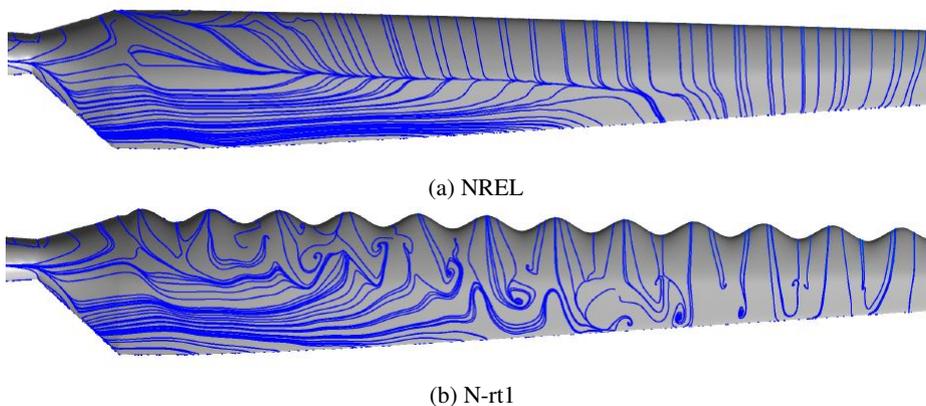

(a) NREL

(b) N-rt1

Figure 4: Velocity streamlines over the upper face of the blades at $10 \ m/s$
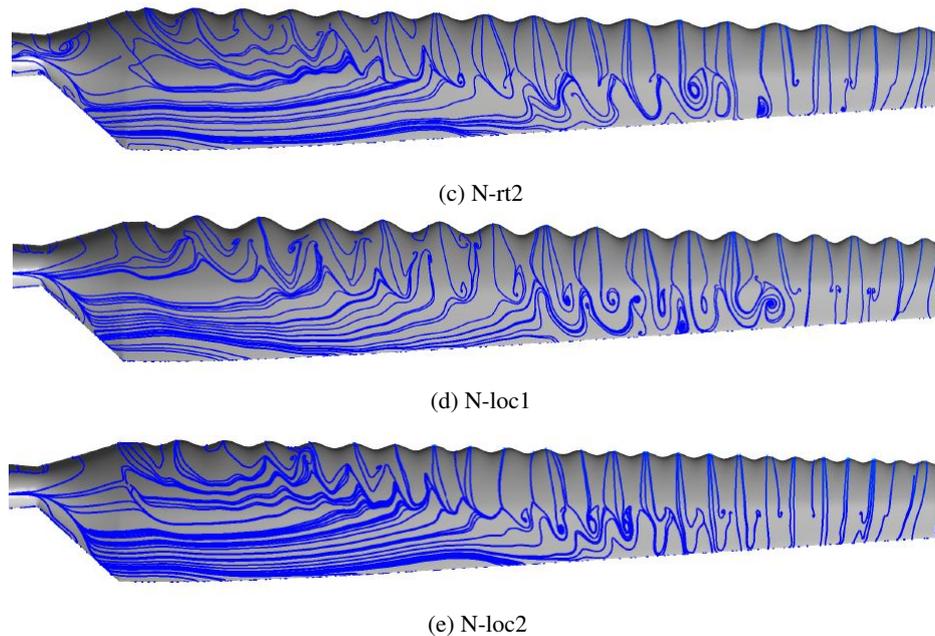
(c) N-rt2

(d) N-loc1

(e) N-loc2

Figure 4: Velocity streamlines over the upper face of the blades at $10\ m/s$ (cont.)

4. Conclusions

The WLE has been proposed as a useful device to enhance the HAWT performance. However, when tested on the NREL Phase VI wind turbine blade, it showed to be efficient only at high improbable wind speeds and to significantly degrade the blade performance at its design wind speed. The WLE effects depend on its governing parameters, A and λ. Therefore, blades designed with the WLE in function to a fixed blade chord makes it efficient only in a section of the blade. In this study, A and λ were set in function to the blade local chord so that the WLE dimensions decrease proportionally to the blade chord. It was possible to achieve a less severe torque reduction at the blade design speed and still increase the blade performance at higher wind speeds. Under this approach it is possible to search for an optimum WLE configuration to extend the blade operational range.

5. Acknowledgments

6. References

Abate, G. and Mavris, D.N., 2018. "Performance analysis of different positions of leading edge tubercles on a wind turbine blade". In *2018 Wind Energy Symposium*. p. 1494.

Abate, G., Mavris, D.N. and Sankar, L.N., 2019. "Performance effects of leading edge tubercles on the nrel phase vi wind turbine blade". *Journal of Energy Resources Technology*, Vol. 141, No. 5, p. 051206.

Bolzon, M.D., Kelso, R.M. and Arjomandi, M., 2016. "Formation of vortices on a tubercled wing, and their effects on drag". *Aerospace Science and Technology*, Vol. 56, pp. 46–55.

Custodio, D.S., 2007. "The effect of humpback whale-like protuberances on hydrofoil performance".

Dropkin, A., Custodio, D., Henoch, C. and Johari, H., 2012. "Computation of flow field around an airfoil with leading-edge protuberances". *Journal of Aircraft*, Vol. 49, No. 5, pp. 1345–1355.

Fish, F.E. and Battle, J.M., 1995. "Hydrodynamic design of the humpback whale flipper". *Journal of Morphology*, Vol. 225, No. 1, pp. 51–60.

Hand, M., Simms, D., Fingersh, L., Jager, D., Cotrell, J., Schreck, S. and Larwood, S., 2001. "Unsteady aerodynamics experiment phase vi: wind tunnel test configurations and available data campaigns". Technical report, National Renewable Energy Lab., Golden, CO.(US).

Hansen, K.L., Kelso, R.M. and Dally, B.B., 2011. "Performance variations of leading-edge tubercles for distinct airfoil profiles". *AIAA journal*, Vol. 49, No. 1, pp. 185–194.

Johari, H., Henoch, C.W., Custodio, D. and Levshin, A., 2007. "Effects of leading-edge protuberances on airfoil perfor-

mance". *AIAA journal*, Vol. 45, No. 11, pp. 2634–2642.

Letcher, T.M., 2017. *Wind energy engineering: a handbook for onshore and offshore wind turbines*. Academic Press.

Manwell, J.F., McGowan, J.G. and Rogers, A.L., 2010. *Wind energy explained: theory, design and application*. John Wiley & Sons.

Menter, F.R., Kuntz, M. and Langtry, R., 2003. "Ten years of industrial experience with the sst turbulence model". *Turbulence, heat and mass transfer*, Vol. 4, No. 1, pp. 625–632.

Miklosovic, D., Murray, M., Howle, L. and Fish, F., 2004. "Leading-edge tubercles delay stall on humpback whale (megaptera novaeangliae) flippers". *Physics of fluids*, Vol. 16, No. 5, pp. L39–L42.

Sobotta, D., Howell, R. and Jing, L., 2016. "Investigating the role of wind turbine pitch using cfd". In *MATEC Web of Conferences*. EDP Sciences, Vol. 59, p. 06004.

Song, Y. and Perot, J.B., 2015. "Cfd simulation of the nrel phase vi rotor". *Wind engineering*, Vol. 39, No. 3, pp. 299–309.

Sørensen, N.N., Michelsen, J. and Schreck, S., 2002. "Navier–stokes predictions of the nrel phase vi rotor in the nasa ames 80 ft× 120 ft wind tunnel". *Wind Energy: An International Journal for Progress and Applications in Wind Power Conversion Technology*, Vol. 5, No. 2-3, pp. 151–169.

Zhang, R.K. and Wu, V.D.J.Z., 2012. "Aerodynamic characteristics of wind turbine blades with a sinusoidal leading edge". *Wind Energy*, Vol. 15, No. 3, pp. 407–424.

7. Responsibility Notice

The authors are the only responsible for the printed material included in this paper.